AD-A078 988 OREGON GRADUATE CENTER BEAVERTON F/G 11/6
EFFECT OF RETAINED AUSTENITE ON HYDROGEN EMBRITTLEMENT OF STEEL--ETC(U)
NOV 79 W E WOOD DAAG29-76-G-0317
UNCLASSIFIED ARO-13894.2-MS NL

END
DATE FILMED
2-80
DDC

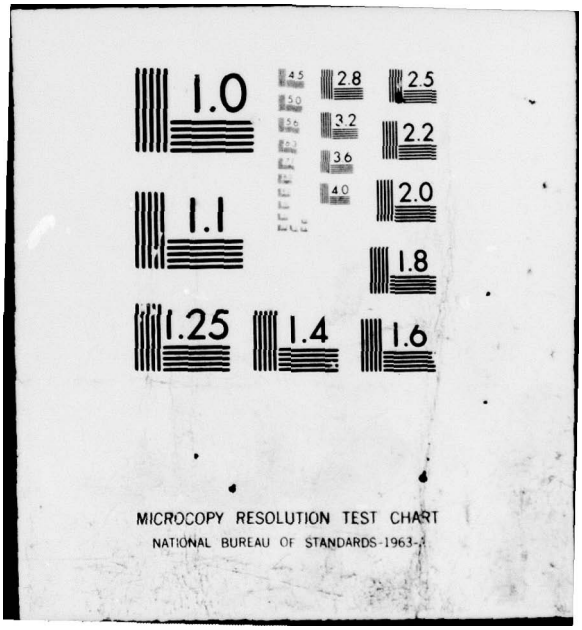
1.0
1.1
1.25
1.4
1.6
1.8
2.0
2.2
2.5
2.8
3.2
3.6
4.0
4.5
5.0
5.6
MICROCOPY RESOLUTION TEST CHART
NATIONAL BUREAU OF STANDARDS-1963-A

EFFECT OF RETAINED AUSTENITE ON HYDROGEN EMBRITTLEMENT OF STEELS

FINAL REPORT

DR. W.E. WOOD

AUGUST 31, 1979

U. S. ARMY RESEARCH OFFICE

DAA G29-76-G-0317
DAA G29-78-G-0158

OREGON GRADUATE CENTER

Unclassified

SECURITY CLASSIFICATION OF THIS PAGE (When Data Entered)

REPORT DOCUMENTATION PAGE

READ INSTRUCTIONS BEFORE COMPLETING FORM

1. REPORT NUMBER

2. GOVT ACCESSION NO.

3. RECIPIENT'S CATALOG NUMBER

(6) 4. TITLE (and Subtitle)

EFFECT OF RETAINED AUSTENITE ON HYDROGEN EMBRITTLEMENT OF STEELS

5. TYPE OF REPORT & PERIOD COVERED

Final Report: 9-1-76 thru 8-31-79

6. PERFORMING ORG. REPORT NUMBER

(10) 7. AUTHOR(s)

W. E. Wood

(12) 18

8. CONTRACT OR GRANT NUMBER(s)

(15) DAA G29-76-G-0317
DAA G29-78-G-0158

9. PERFORMING ORGANIZATION NAME AND ADDRESS

Oregon Graduate Center
19600 NW Walker Road
Beaverton, Oregon 97005

390 077

10. PROGRAM ELEMENT, PROJECT, TASK AREA & WORK UNIT NUMBERS

11. CONTROLLING OFFICE NAME AND ADDRESS

U. S. Army Research Office
P. O. Box 12211
Research Triangle Park, NC 27709

(11) 12. REPORT DATE

14 Nov 79

13. NUMBER OF PAGES

16

(9) 14. MONITORING AGENCY NAME & ADDRESS (if different from Controlling Office)

Final rept. 1 Sep 76-31 Aug 79.

15. SECURITY CLASS. (of this report)

Unclassified

15a. DECLASSIFICATION/DOWNGRADING SCHEDULE

16. DISTRIBUTION STATEMENT (of this Report)

Approved for public release; distribution unlimited.

(18) ARO (19) 13894.2-MS

17. DISTRIBUTION STATEMENT (of the abstract entered in Block 20, if different from Report)

18. SUPPLEMENTARY NOTES

The view, opinions, and/or findings contained in this report are those of the author(s) and should not be construed as an official Department of the Army position, policy, or decision, unless so designated by other documentation.

19. KEY WORDS (Continue on reverse side if necessary and identify by block number)

Hydrogen embrittlement, microstructure, low alloy steel, grain size, retained austenite, threshold stress intensity, crack growth rates.

20. ABSTRACT (Continue on reverse side if necessary and identify by block number)

Ultrahigh strength steel alloys heat treated to 200,000 psi yield strength levels are notoriously sensitive to hydrogen induced delayed failure. In this program the effects of microstructure, especially that of retained austenite, on hydrogen induced (a) threshold stress intensity level, (b) crack growth rate, and (c) fatigue crack growth rate have been investigated. Microstructural variables investigated included prior austenite grain size, twinning, carbides, retained austenite, and indirectly, segregation. Emphasis in this study has

DD FORM 1 JAN 73 1473 EDITION OF 1 NOV 65 IS OBSOLETE

Unclassified 390 077

SECURITY CLASSIFICATION OF THIS PAGE (When Data Entered)

ABSTRACT

Ultrahigh strength steel alloys heat treated to 200,000 psi yield strength levels are notoriously sensitive to hydrogen induced delayed failure. In this program the effects of microstructure, especially that of retained austenite, on hydrogen induced (a) threshold stress intensity level, (b) crack growth rate, and (c) fatigue crack growth rate have been investigated. Microstructural variables investigated included prior austenite grain size, twinning, carbides, retained austenite, and indirectly, segregation. Emphasis in this study has been placed on the contribution of and stability of retained austenite.

Optical, scanning electron microscopy, and transmission electron microscopy have been employed to establish microstructural details. Compact tension and bolt loaded fracture toughness specimens were used throughout the program. Precision hydrogen measurements were carried out by the Boeing Company. It was necessary to measure the hydrogen content for each sample, since it was not possible to introduce consistent hydrogen levels by cathodically charging. The influence of retained austenite is limited by its instability at the crack tip, where it has been shown to transform due to the intense stresses and strains in the plastic zone.

Acoustic emission analysis was employed to detect and study the microscopic nature of crack growth as well as to establish a threshold stress intensity level. Test results showed that retained austenite, grain size, and probable segregation each contribute towards altering the hydrogen induced delayed failure characteristics.

INTRODUCTION

Sustained load cracking at stress intensity levels well below K_{Ic} typifies internal hydrogen embrittlement in low alloy steels heat treated to high strength levels. At or near a crack tip hydrogen exerts an embrittling effect that leads to intergranular, transgranular, or mixed mode fracture[1], all of which exhibit drastically reduced macroscopic ductility. Proposed mechanisms include a decohesion model [2,3], dislocation mobility[4] and surface energy considerations[5,6], stress-sorption[7], and planar pressure theories[8,9,10]. In

the specific case of internal hydrogen embrittlement the atomic hydrogen migrates to the crack tip under the influence of a triaxial stress state[2,11,12], and for each of the above models the amount of and mobility of atomic hydrogen thus play key roles in the hydrogen induced delayed brittle failure[1-8,11,12].

The microstructure of BCC steel strongly influences mobility of dissolved hydrogen. In Coe and Martin's[13] review of microstructural effects on apparent hydrogen diffusivity in steel they reported that iron carbide present in globular form allows apparent diffusivity one order of magnitude greater than when the carbides form a coarse pearlite structure. Others have shown that martensite and lower bainite have very low diffusivities, apparently due to finely dispersed autotempered carbides in the strained lattice.[14,15]

McNab and Foster[16] developed a model assuming hydrogen to be delayed at specific sites in the lattice due to the presence of potential wells significantly deeper than those encountered in normal regions of a crystal lattice. Oriani[17] expanded this model to show that dissolved hydrogen is trapped or delayed even when it diffuses within a small distance of a trap. Using a similar trapping model Evans and Rollason[18] studied the effects of voids on apparent hydrogen diffusivity in a high sulphur, free cutting steel and concluded that apparent diffusivity could be decreased by an order of magnitude through a trapping mechanism.

Several investigators have suggested that trapping of hydrogen at specific sites in the lattice should improve resistance to hydrogen induced delayed cracking by immobilizing the atomic hydrogen[19-28]. Kortovich[20] showed that rare earth additions of cerium and lanthanum in AISI 4340 steel led to increased threshold stress intensities and lower crack growth rates in cathodically charged specimens. Cedeno[27] and Ritchie et al.[29] found that a Si modified 4340 steel containing significant quantities of retained austenite exhibited reduced crack growth rates when compared with an unmodified 4340 alloy. However, they found that the threshold stress intensities remained relatively unchanged. Additionally, while retained austenite has been shown to be thermally stable, its stability during deformation and its stability in the presence of hydrogen is not clear.

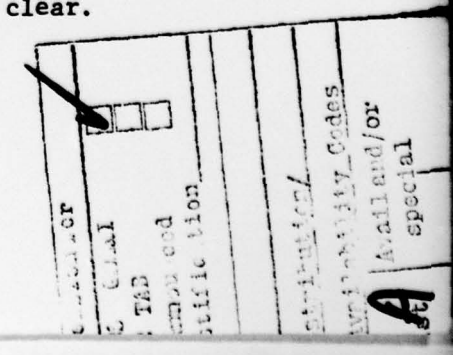

The present study established microstructural effects on the hydrogen induced failure characteristics of commercial 4340 steel heat treated to the 200,000 psi yield strength level. Both internal and external hydrogen embrittlement analysis has been carried out. Fundamentally, the hydrogen distribution and its general availability is different in each case.

EXPERIMENTAL METHODS

The material used in this investigation was aircraft quality commercial AISI 4340 steel received in the fully annealed condition. The as-received material was machined into bolt loaded double cantilever beam (DCB) and compact tension test specimens. The specimens were then degreased and vacuum annealed at 500°C for 8 hours at a pressure of 10^{-7} torr in an ion-pumped system.

Heat treatment schedules (See Table I) included a 1 hour solution treatment in an argon atmosphere at either 870°C or 1200° followed by direct oil quenching to room temperature. A step quenching procedure consisting of 870°C for 1/2 hour prior to direct oil quenching was also employed. Salt bath tempering for 1 hour at either 180°C or 280°C followed each solution treatment. These heat treatments are discussed elsewhere[31-33] and the tensile and K_{Ic} data[32] are presented in Table II.

Following heat treatment all samples were polished and cathodically charged with hydrogen at 25°C in a 4% sulphuric acid bath containing a poison consisting of 1 gm yellow phosphorus dissolved in 20 ml. of carbon disulphide (CS_2). Each bath contained 600 ml. of the acid solution and 10 ml of the poison mixture. The charging current density was 14 mA/cm^2 and the charging time was varied from 6 hours to 48 hours to facilitate varying degrees of hydrogen ingestion in the test samples.

Immediately following the charging operation each specimen was hand polished using 300 grit emery cloth and ultrasonically cleaned for 10 minutes in a 10% HCl solution. After rinsing the specimens were cadmium plated in a cyanide plating bath at a current density of 2.5 A/cm^2 for 10 minutes.

Hydrogen measurements were conducted by utilizing an "Ultrasensitive Hydrogen Analysis System" developed by K.B. Das.[29,30] This instrument allows the measurement of hydrogen content in the range of a few parts per billion

in a carrier gas stream of argon, and is proven to have the capability of measuring relative hydrogen contents in metals of the order of a few tenths ppm with an accuracy of better than $\pm$ 10%. This analysis capability was necessary for hydrogen measurements in this study, since reportedly the presence of only few ppm (by weight) nascent hydrogen can embrittle high-strength steels. Details regarding operating procedure, range, and accuracy of the instrument are described elsewhere.[30]

Threshold stress intensities were established using bolt loaded specimens. Sustained load and fatigue crack growth rates were determined using a compact tension specimen. Crack length measurements were carried out by a compliance measurements, C.O.D. gage and an optical microscope. Fatigue tests were carried out at 10 Hz under semisoidal tension at a load ratio, R = 0.25.

Acoustic emission analysis was carried out to establish the nature of crack growth on a microscopic scale. Total counts, events, amplitude distribution, and frequency analysis was performed under static load conditions.

SUMMARY OF RESULTS

Hydrogen Analysis

Fig. 1 shows dissolved hydrogen content as a function of charging time for heat treatment A. Although hydrogen pick-up tended to increase with increasing charging time in general, the scatter in the data clearly shows why one should not attempt to predict accurate hydrogen levels[34] based on charging time alone. This ambiguity points out the danger inherent in the application of calculated hydrogen concentrations to studies of internal hydrogen induced cracking.

Furthermore as received material contained as much as 2.5 ppm hydrogen. Vacuum annealing, while lowering this content to under 1 ppm, required careful control to result in reproducible hydrogen levels.

Threshold Stress Intensity Levels

For the case of internal hydrogen embrittlement, IHE, Fig. 2 summarizes the threshold data as a function of hydrogen content, and Table III

presents an analysis of microstructure and mechanical properties associated with each microstructure studied. Microstructural contributions controlling the threshold stress intensity levels may be summarized as follows:

1. Redistribution of impurities such as phosphorus and sulphur in a more homogeneous manner led to an increase of ~3.5 MP a$\sqrt{m}$ in the baseline K_{th} of the present steel.

2. An increase in grain diameter from 15-20 microns to 150-200 microns led to a baseline K_{th} increase of 5.5 MP a$\sqrt{m}$.

3. An increase in the amount of retained austenite present as a fine interlath distribution led to a baseline K_{th} increase of ~9MP a$\sqrt{m}$.

4. Threshold stress intensity values varied greatly with specimen dissolved hydrogen contents between 1 ppm and 2 ppm. At dissolved hydrogen levels above ~2.5 ppm a baseline K_{th} value independent of dissolved hydrogen content was attained.

For the case of external hydrogen embrittlement, similar heat treatments resulted in approximately the same threshold stress intensities as did the internally charged specimen. Hence from a threshold standpoint the coarse grained structure containing retained austenite resulted in the highest threshold stress intensity levels.

Crack Growth Rate Analysis

Crack growth rate analysis was performed for (1) sustained load under internal (IHE) and external (HEE) conditions and (2) fatigue load under IHE conditions. Figure 3 is representative of the type of data obtained, and Table IV and Figure 4 summarize the data. Again the coarse grained structure containing retained austenite exhibited not only the lowest crack growth rates, but also a greatly extended stage II region crack growth. In fact the conventional specimens would have failed due to K_{Ic} load conditions whereas the coarse grained specimen would still be exhibiting stable crack growth.[32]

Contrary to IHE conditions, external hydrogen embrittlement (HEE) resulted in crack growth rates that were basically unaffected by microstructure in the stage II region. Crack growth rates were all about 10^{-4} in/sec.

Fatigue crack growth rate analysis was carried out for the same heat treatment and thus microstructural conditions. Tests were performed for the internal hydrogen case only. The results shown in Figure 5 compare tests done in air to those cathodically charged. In the uncharged condition the curves are identical in the lower stress intensity range. However, as the stress intensity increased the coarse grained specimens exhibited improved crack growth resistance. For the case of internally charged specimens increased crack growth was generally observed. However, at low applied stress intensities the coarse grained material exhibited a fatigue threshold identical to uncharged specimens, while the fine grain specimen exhibited accelerated crack growth and no apparent threshold levels. In the presence of internal hydrogen, in no case was the performance of the coarse grained structure containing retained austenite worse than that of the conventional fine grain material.

Stability of Retained Austenite

All the tests conducted under this program have supported the concept of improved hydrogen embrittlement cracking resistance due to thin films of retained austenite. An important question then is the stability of retained austenite at the crack tip. Hence a extensive careful TEM analysis has been carried out as part of this program.[35] Sections from within the plastic zone of fracture toughness specimens have been examined. Sections removed were as shown in Figure 6 and 7.

In every case extensive twinning was found in the plastic zone and very little, if any, retained austenite was present. Hence retained austenite is not stable under conditions which exist at the crack tip. This is true for monotonic and cyclical loading conditions.

Acoustic Emission Analysis

Acoustic emission studies have shown that, for both external and internal hydrogen embrittlement conditions, individual crack jumps are a function of grain size, if not equivalent to the prior austenite grain size. The amplitude of acoustic events was much larger for coarse grained material. Thus the cracking is dependent on the distribution of crack initiation sites. Additionally, and most important, since the average amplitude emission increased with increasing grain size, the detectability rapidly increased. In

fact, it was impossible to detect cracking at threshold stress intensity levels characteristic of the fine grained 4340 used in this study. This suggests a real danger in utilization of A.E. for stress emission cracking detection in fine grained materials whose crack advancement mechanism is intergranular. Furthermore, the application of AE data and experience to other materials with varying grain sizes may produce widely varying results and significant errors.[36]

CONCLUSIONS

1. For internal hydrogen embrittlement, retained austenite and large grain sizes tend to increase the threshold and decrease the sustained crack growth rates in 4340 steel.

2. For internal hydrogen embrittlement, retained austenite and large grain sizes improved the high cycle fatigue resistance of 4340 equivalent to that of uncharged samples treated in air. Low cycle fatigue rates were unaffected by microstructure when tested in an internal hydrogen environment.

3. Retained austenite is unstable in the crack tip plastic zone as evidenced by transmission electron microscopy analysis.

REFERENCES

1. J.M. Bernstein, R. Garber and G.M. Pressouyre, Effect of Hydrogen on Behavior of Materials, ed. A.W. Thompson and I.M. Bernstein, AIME, (1976), pp 37.
2. A. R. Troiano, Trans. ASM (1960), 52, 54.
3. R.A. Oriani, Ber. der Bunsen-Gessell. (1972), 76, 848.
4. P. Bastien and P. Azou, Rev. Met. (1952), 49, 837.
5. N. Petch, Phil. Mag. (1956), 1, 331.
6. N. Petch and P. Stables, Nature (1952), 169, 842.
7. H. Uhlig, Physical Metallurgy of Stress Corrosion Fracture, Interscience New York (1959).
8. A. S. Tetelmann and A.J. McEvily, Fracture of Structural Materials, Wiley, New York (1967).
9. H. G. Nelson, D.P. Williams and A.S. Tetelman, Met. Trans. (1971) 2, 953.
10. C. Zapffe, Trans. ASM (1947), 39, 191.
11. W.D. Benjamin and E. A. Steigerwald, Met. Trans. (1971), 2, 606.
12. H. P. VanLeeuwen, Corrosion (1973), 29, 197.
13. F. R. Coe and J. Martin, Met. Sci. J. (1969), 3, 209.
14. M. Smialouski, Hydrogen in Steel, Pergamon Press (1962).
15. U. V. Bhat and H. K. Lloyd, J.I.S.I. (1952), 165, 382.
16. A. M. McNabb and P. K. Foster, Trans. Met. Soc. AIME (1963), 227, 618.
17. R. A. Oriani, Fundamental Aspects of Stress Corrosion Cracking, ed. Staehl, Forty, Van Rooyen, NACE 32 (1967).
18. G. M. Evans and E. C. Rollason, JISI (1969), 207, 1591.
19. W. W. Gerberich and F. J. Lessar, Met. Trans. (1976), 7A, 953.
20. C. S. Kortovich, ER 7814-2, TRW Equip. Mat. Tech., Cleveland, Ohio (1977).
21. B. D. Craig, Acta Met. (1977), 25, 1027.
22. P. A. Parrish, K. B. Das, and W. E. Wood.
23. R. Gibala, ASME Abstr. Bull. (Inst. Met. Div.) (1966), 1, 36.
24. L. S. Darken and R. P. Smith, Corrosion (1949), 5, 1.
25. E. W. Johnson and M.L. Hill, Trans. Met. Soc. AIME (1960) 218, 1104.
26. G. Maeser and N. Dautzenberg, Arch, Eisenhuttenw. (1965), 36, 175.
27. M. H. C. Cedeno, Master's Thesis, Univ. Calif. Berkeley (1977).
28. R. O. Ritchie, M. Y. C. Cedeno, V. F. Zackay and E. R. Parker, Met. Trans. (1978) 9A, 35.
29. K. B. Das and W. E. Strobelt, U. S. Patent #3783678 (1974).
30. K. B. Das, Hydrogen in Metals, ed. M. Bernstein and A.W. Thompson, ASM (1974), pg. 690.
31. G. Y. Lai, W.E. Wood, R.A. Clark, V.F. Zackay and E.R. Parker, Met. Trans. (1974) 5, 1663.
32. W. E. Wood, NASC Final Tech. Report N00019-77-C-0135, (1978).
33. K. H. Khan and W. E. Wood, Met. Trans. (1978) 9A 899.
34. C. E. Bauer, K. B. Das, and W. E. Wood, unpublished research.
35. C. N. Sastry, K. H. Khan, W. E. Wood, "Mechanical Stability of Retained Austenite in Quench and Tempered 4340 Steel", to be presented at 109th AIME Annual Meeting, Las Vegas, Nevada, Feb. 1980.
36. D. Dilipkumar, W.E. Wood, "A New Approach to Acoustic Emission Analysis", presented at Fall 1979 AIME meeting, Milwaukee, Wis.

PERSONNEL SUPPORTED DURING THE PROGRAM

1. W. E. Wood - Principal Investigator, Assoc. Prof.
2. K. Khan - Post Doctoral Research Fellow
3. K. B. Das - Boeing Aerospace Company
4. C. Bauer* - Graduate Student Research Asst.
5. C. Dilipkumar** - Graduate Student Research Asst.
6. C. Sastry** - Graduate Student Research Asst.

* Ph.D. thesis completed

** Ph.D. thesis partially completed under this grant

GRANT RELATED PUBLICATIONS

W. E. Wood, Influence of Microstructure on Hydrogen Embrittlement in High Strength Steel, presented at the 3rd International Conference on Hydrogen in Metals, Paris, France 1977.

C. Bauer, W.E. Wood, Effect of Austenitizing Temperature on Hydrogen Induced Failure in High Strength Low Alloy Steel, accepted for publication in Met. Trans.

W. E. Wood, D. Dilipkumar, A Composite Grip Design for Elimination of Extraneous Noise During Acoustic Emission Testing, J. Test. and Eval. 6, No.6 369-370 (1978).

D. Dilipkumar, W.E. Wood, Acoustic Emission Analysis of Fracture Toughness Testing, presented at the 1979 SESA Spring meeting, San Francisco 1979, accepted for publication in J. Test. & Eval.

W. E. Wood, D. Dilipkumar, V.S. Rao Gudemetia, Amplitude-Distribution Analysis of Acoustic Emission, presented at the 1979 SESA Spring meeting, San Francisco, 1979, accepted for publication in J. Test. & Eval.

C. N. Sastry, K. Khan, W. Wood, Precipitation of Cementite on Twins in Low Alloy Steels, 37th Ann. Proc. Electron Microscopy Soc. Amer, 1979.

C. E. Bauer, W.E. Wood, K. Das, Microstructural Effects on the Hydrogen Embrittlement of 4340 Steels, ibid. 1979.

D. Dilipkumar, W.E. Wood, A New Approach to Acoustic Emission Analysis, ibid. 1979.

C.N. Sastry, K.H. Khan and W.E. Wood, Mechanical Stability of Retained Austenite in Quenched and Tempered AISI 4340 steel, to be presented at the 109th AIME meeting in Las Vegas, Nev., Feb. 1980.

D. Dilipkumar, W.E. Wood,"A New Approach to Acoustic Emission Analysis",presented at Fall 1979 AIME meeting, Milwaukee Wis.

TABLE I

Heat Treatment Schedules

Heat Treatment	Solution Treatment	Tempering Treatment
A	1200°C 1 hr. oil quench	180°C 1 hr.
B	1200°C 1 hr. oil quench	280°C 1 hr.
C	1200°C 1 hr. furnace quench to 870°C 1/2 hr. oil quench	180°C 1 hr.
D	1200°C 1 hr. furnace quench to 870°C 1/2 hr. oil quench	280°C 1 hr.
E	870°C 1 hr. oil quench	180°C 1 hr.
F	870°C 1 hr. oil quench	280°C 1 hr.

TABLE II

Mechanical Properties and Plane Strain Fracture Toughness as a Function of Heat Treatment

Heat Treatment	σ_{ys} (MPa)	σ_{ult} (MPa)	Elong.(%)	R.A.(%)	K_{IC} (MPa$\sqrt{m}$)
A	1551	1931	4.5	7.1	99.23
B	1448	1655	1.2	4.5	68.24
C	1586	2069	7.1	13.0	69.50
D	1448	1793	7.3	16.5	57.85
E	1520	2000	13.6	40.2	65.71
F	1517	1655	13.7	53.7	83.84

TABLE III

Microstructural Features Mechanical Property and Threshold Hydrogen Embrittlement Characteristics as a Function of the Heat Treatment Variables

Tempering Temperature	SOLUTION TREATMENT		
	1200°C	1200°C/870°C	870°C
	A	C	E
180°C	Retained γ Relatively homogeneous impurity distribution No twinning Grain diameter 150-200μm K_{IC} 99.23 MPa √m K_{th} 39.25 MPa √m σ_{ys} 1515 MPa	Retained γ Grain boundary impurity segregation Extensive twinning Grain diameter 150-200μm K_{IC} 69.5 MPa √m K_{th} 26.5 MPa √m σ_{ys} 1526 MPa	No retained γ Grain boundary impurity segregation Extensive twinning Grain diameter 15-20μm K_{IC} 65.7 MPa √m K_{th} 12.0 MPa √m σ_{ys} 1520 MPa
	B	D	F
280°C	No retained γ Relatively homogeneous impurity distribution No twinning Grain diameter 150-200μm K_{IC} 68.24 MPa √m K_{th} 21.0 MPa √m σ_{ys} 1448 MPa	No retained γ Grain boundary impurity segregation Extensive twinning Grain diameter 150-200μm K_{IC} 57.9 MPa √m K_{th} 17.5 MPa √m σ_{ys} 1448 MPa	No retained γ Grain boundary impurity segregation Extensive twinning Grain diameter 15-20μm K_{IC} 83.9 MPa √m K_{th} 12.0 MPa √m σ_{ys} 1517 MPa

Microstructural Features as a Function of the Heat Treatment Variables

TABLE IV

Stage II Hydrogen Embrittlement Sustained Load Crack Growth Rates

HEAT TREATMENT		$\frac{da}{dt}$ (in sec $^{-1}$)	H (ppm by wt)
1200/180	A	3.7×10^{-6}	2.32
1200/280	B	2.8×10^{-5}	2.75
1200/870/180	C	3.4×10^{-6}	3.00
1200/870/280	D	4.0×10^{-5}	2.65
870/180	E	2.0×10^{-5}	2.89
870/280	F	4.8×10^{-6}	3.25

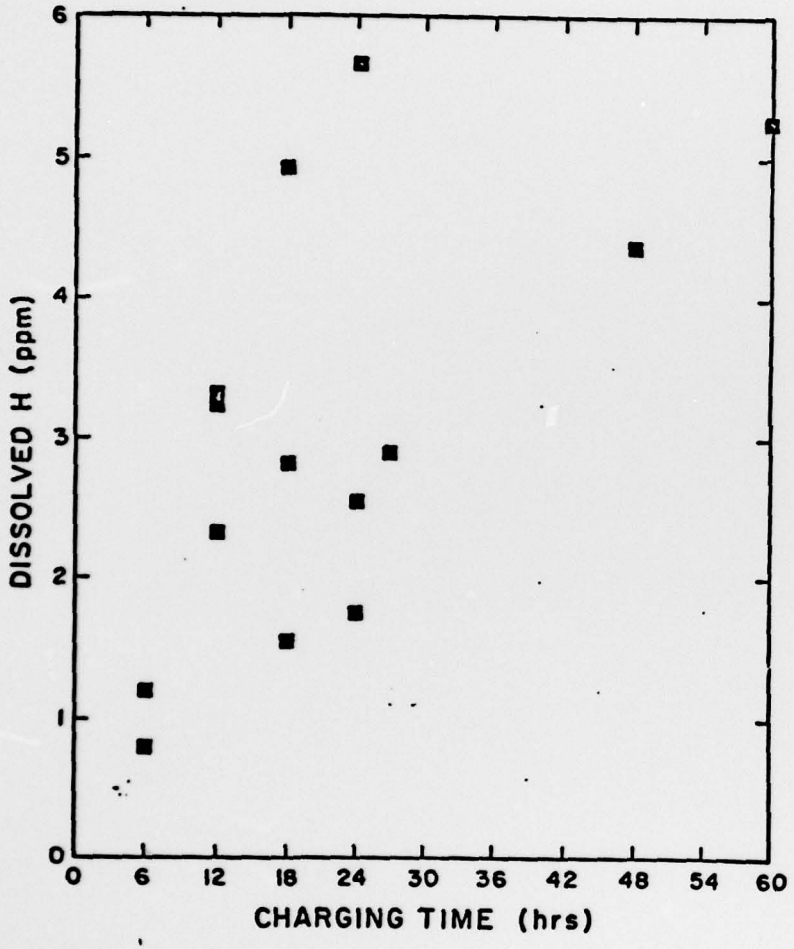

Figure 1. Dissolved hydrogen content as a function of charging time for 1200°C austenitized specimens tempered at 180°C

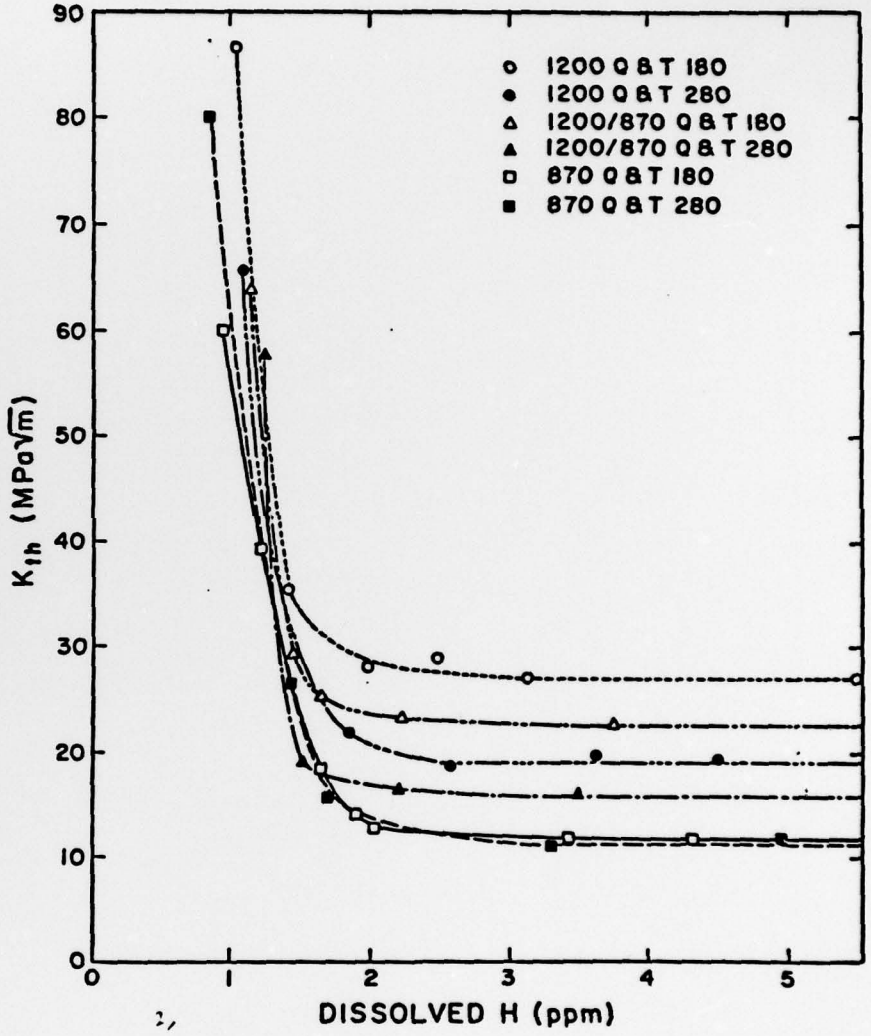

Figure 2. Threshold stress intensity versus hydrogen content and heat treatment.

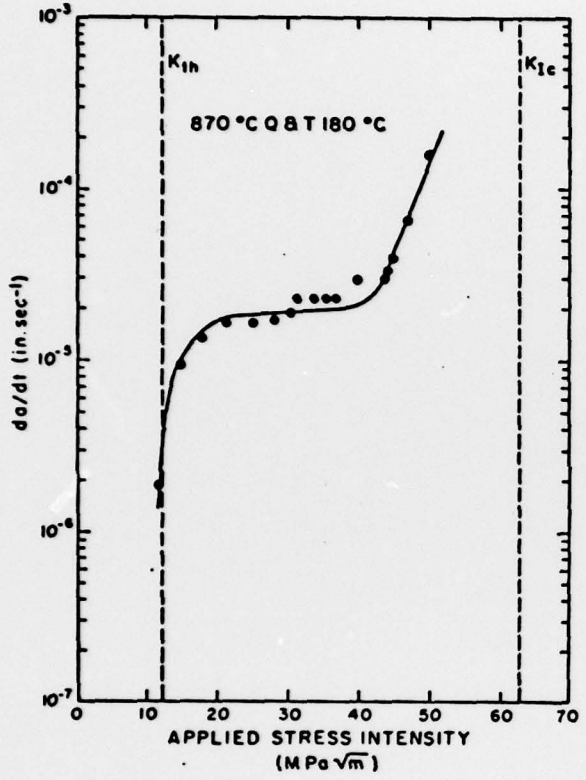

Figure 3. Typical crack growth rate curves for cathodically charged specimens.

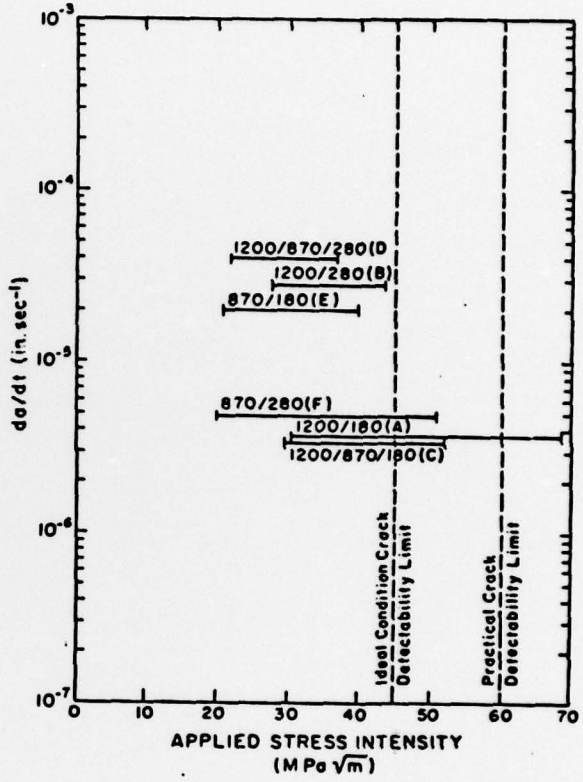

Figure 4. Sustained load stage II crack rates for cathodically charged specimens as a function of heat treatment. See Table III for microstructural details.

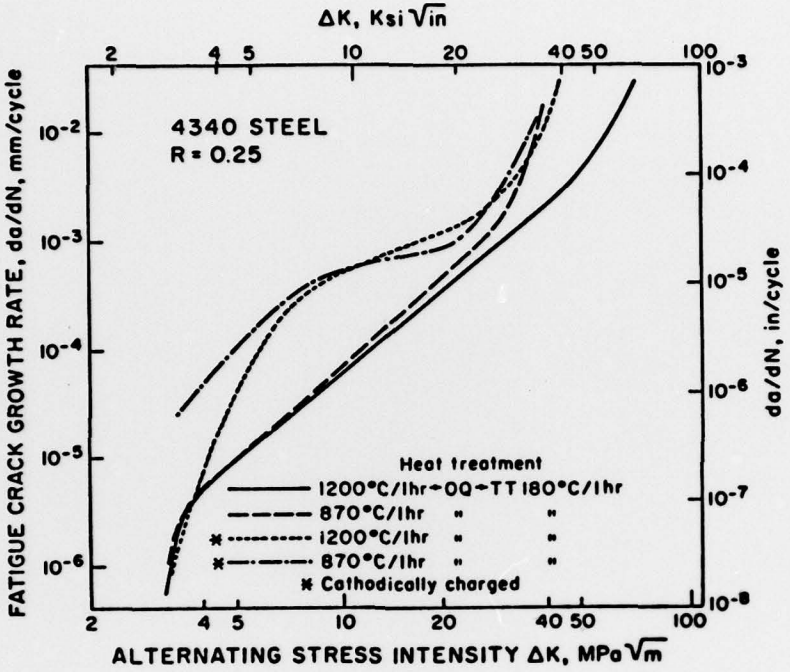

Figure 5. Fatigue crack growth rate as a function of heat treatment and hydrogen content. See Table III for corresponding microstructural details.

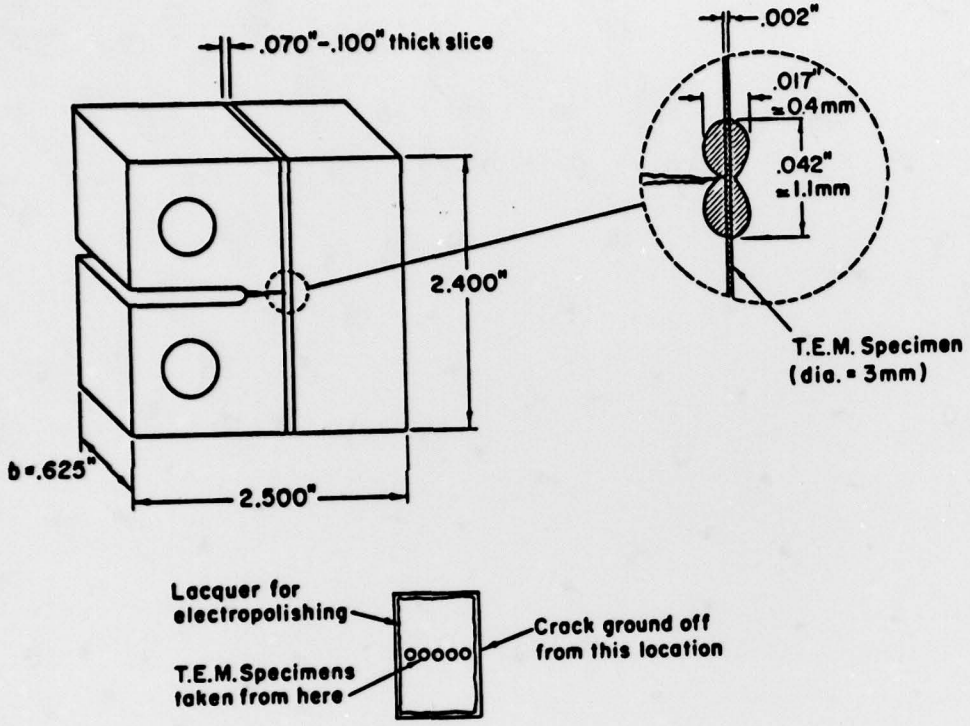

Figure 6. Schematic illustration of specimen sectioning for transmission electron microscopy analysis.

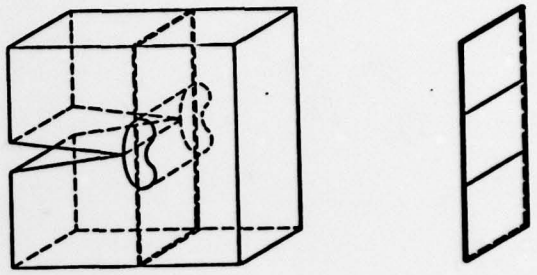

Figure 7. Schematic illustration showing TEM section as removed from the plastic zone.